Effect of Roll Gap Change of Oval Pass on Interfacial Slip of Workpiece and Roll Pressure in Round-Oval-Round Pass Rolling Sequence

Laila Salah Bayoumi
Department of Mechanical Design and Production, Cairo University, Giza, Egypt
Youngseog Lee*
Plate, Rod & Welding Group and Steel Products & Process Group at POSCO Technical Research Laboratories, Pohang, Kyungbuk 790-785, Korea
Hong Joon Kim
Steel Products & Process Group at POSCO Technical Research Laboratories, Pohang, Kyungbuk 790-785, Korea

This paper presents a study of the effect of varying the roll gap of oval pass in round-oval-round pass sequence on the interfacial slip of workpiece, entrance and exit velocities, stresses and roll load that the workpiece experiences during rolling, by applying analytical method, finite element simulation and verification through hot bar rolling tests. The results have shown that the roll gap variation of oval pass affects the interfacial slip of workpiece along the groove contact and the specific roll pressure. The optimum conditions in terms of minimum interfacial slip and minimum specific roll pressure, which might influence the maximum groove life, is obtained when the subsequent round pass is completely filled.

Key Words : Rod Rolling, Analytical Solution, Interfacial Slip, Roll Pressure

Nomenclature

a_r : Torque arm ratio
A_e : Profile cross sectional area
A_s : Projected area of roll contact
$2b$: Profile central width
$2b_s$: Width of contact at exit
c : Slip coefficient
e : Centroid height of half exit sectional area
$2g$: Oval pass roll gap
$2h$: Profile central height
$2h_s$: Height of contact at exit
L : Length of roll contact
m : Friction factor
q : Stress coefficient
p : Surface pressure
p_s : Specific roll pressure
P : Roll load
r_g : Groove radius
r_n : Neutral roll radius
r_s : Profile side radius
$2r_c$: Rolls center distance
$2r_i$: Roll inner diameter
$2r_o$: Roll outer diameter
s_i : Slip at roll inner diameter
T : Rolling torque
v_e : Workpiece exit velocity
$\bar{\varepsilon}$: effective strain
v_i : Workpiece velocity at inner roll radius
v_o : Workpiece entry velocity
$\dot{\bar{\varepsilon}}$: Effective strain rate
$\bar{\sigma}$: Flow stress
ω : Roll angular velocity
μ : Coefficient of friction

* Corresponding Author,
E-mail : pc554162@posco.co.kr
TEL : +82-54-220-6058; **FAX** : +82-54-220-6911
Plate, Rod & Welding Group at POSCO Technical Research Laboratories, Pohang, Kyungbuk 790-785, Korea. (Manuscript **Received** July 24, 2001; **Revised** December 17, 2001)

σ_θ : Tangential stress
τ : Shear traction

1. Introduction

The round-oval-round roll pass sequence constitutes the intermediate and finishing passes for the production of rounds in continuous rod (or bar) rolling lines. It has the merits of simple geometry, easy manipulation in guides, uniform deformation and good surface quality free from folds. The design of such pass sequence, as well as other passes, and the prediction of entrance and exit velocities, roll load and torque have been until recently empirical (Wusatowski, 1969; Teslikov et al., 1981 ; Arnold and Whitton, 1975) During the last two decades several theoretical and experimental studies have been carried out which enabled replacing the empirical approach by finite element method (Park and Oh, 1990; Shin et al., 1992; Komori, 1997) and/or analytical method (Bayoumi, 1998).

The design of a round-oval-round roll pass sequence is sensitive to the calibration of roll gap in the oval pass since it affects seriously the workpiece profile (exit cross sectional shape), roll load and torque. Maintaining the roll gap of the round pass unchanged, and increasing the roll gap of the oval pass will cause overfilling of the subsequent round pass whereas decreasing the oval pass roll gap will cause round pass underfilling. It is the aim of the present work to study the effect of varying the roll gap of oval pass in round-oval-round pass sequence on the workpiece profile, entrance and exit velocities, stresses, roll load and torque by applying analytical methods, finite element method and verification through performing hot rolling tests. The results obtained would be helpful in optimum design of pass schedule and could be of potential use in on-line process control of rod (or bar) mill.

In what follows we describe the formulation procedure for the analytical method (Bayoumi, 1998) and finite element method briefly. Then, compared are solutions obtained from the analytical method and finite element method (Kim et al., 2000).

2. Analytical Solution

A flowline field solution was obtained for the analysis of flow and stresses in the workpiece bite zone pass in round-oval-round roll pass sequence (Bayoumi, 1998). The solution is based on relationship of the workpiece velocity to the roll groove surface velocity that a neutral radius r_n should exist for which the workpiece exit velocity v_e is equal to the roll surface velocity so that $v_e = \omega r_n$, where ω is the angular velocity of the roll. The neutral radius r_n is obtained from the constant volume flow condition of linear distribution of workpiece velocity along the roll radius, which by integration yields $r_n = r_c - e$, where e is the centroid height of half the exit sectional area and $2r_c$ is the rolls center distance. The strain rate components are derived by differentiating the velocity components, and the stresses are obtained by combining the material constitutive law with Levy-Mises flow rule and integrating the equations of equilibrium. The solution involves the determination of two coefficients; a slip coefficient c and a stress coefficient q, which are obtained by imposing static and friction boundary conditions. The results obtained from analytical solution in the present work comprise of workpiece velocity field, roll load and torque and stress distribution along the workpiece- roll groove interface.

3. Finite Element Solution

Since plastic deformation behavior varies sensitively with the magnitude of friction at the tool-workpiece interface, it is essential to implement a friction model properly in the finite element formulation. Concerning the modeling of friction at the sliding zone, constant shear friction model may not be suitable in the sense that it does not support our daily experience that friction is reduced as normal pressure decreases. The use of this type of friction model should be limited to the forming processes in which normal pressure does not vary significantly along the interface. The above arguments naturally led us to select the Coulomb friction model in the finite element formulation.

Thus, a sound implementation of the Coulomb friction model requires the proper estimation of the normal pressure acting on the roll and workpiece interface. Developed for this purpose was a penalty finite element method which treats the contact boundary condition (Kim et al., 2000). Finite element formulation for the steady-state analysis of incompressible material has been established to calculate workpiece profile and entrence and exit velocities. The initial temperature condition of the workpiece for FE simulation at each pass was here assumed to be isothermal. The Coulomb friction coefficient was set up as 0.35. It was assumed that the effective strains before entering each pass was zero.

4. Experiment

4.1 Rolling equipment and specimen preparation

A single stand two-high laboratory mill was employed, driven by 75kW constant torque, DC motor. Ductile Cast Iron rolls were used, with 310mm maximum diameter and 320mm face width. The rolling speed was set at 34rpm. A box type furnace with the maximum working temperature of 1400℃ was employed to heat up the specimens to the desired rolling temperature. Low carbon steel with a chemical composition of Fe-0.1C-0.45Mn-0.25Si (wt.%) was used. The material was obtained in the form of square as-cast billet with a side length of 160mm. The specimens to be rolled were cut and machined into a round bar with 60mm diameter and 300mm length.

4.2 Experimental procedure

For the hot rod rolling experiments, specimens were soaked at 1030℃ for 1 hour to ensure a homogenous temperature distribution. They were taken out of the furnace and, when the center temperature of specimens reached 1000℃, the tests were conducted. In order to measure the rolling temperature of workpiece, a thermocouple (type K) with 1.6mm diameter was embedded in 50mm deep holes drilled in the tail ends of the specimen. Entsance guides were installed in front of the roll groove to minimize sideway bending of

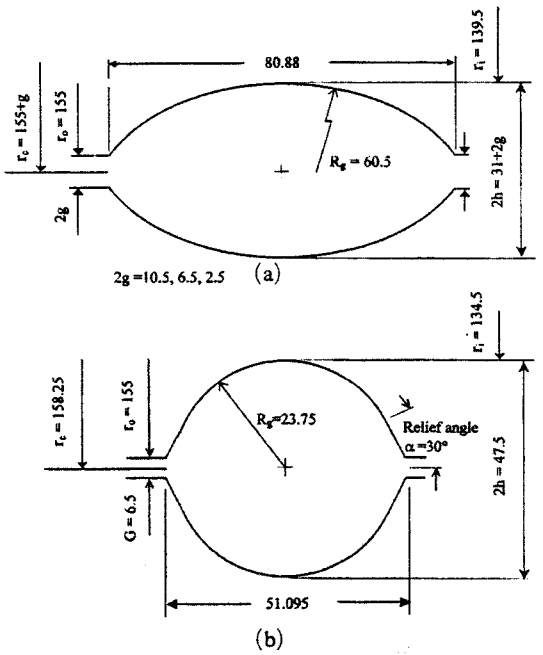

Fig. 1 Two-pass hot bar rolling sequence employed in the experiment
(a) Oval pass and (b) Round pass

specimen. The roll has a round groove and an oval groove as shown in Fig. 1.

A specimen was first rolled into the oval pass, Fig. 1(a), at the desired temperature and cooled in air to room temperature. For the round pass rolling, the workpiece was re-heated up to the desired temperature in the furnace. The oval shape workpiece was then rolled into the round pass, Fig. 1(b), after it was rotated 90 degrees about its axis.

The roll gap of the round pass was maintained unchanged at 6.5mm throughout the study whereas the roll gap of the oval pass had the consecutive values of 10.5, 6.5 and 2.5mm. The roll force was measured by using two force transducers during rolling, located over the bearing blocks of the top work roll. To assure the credibility of experimental data, the experiment was repeated three times under the same rolling condition.

5. Results and Discussion

5.1 Workpiece profile

Figures 2 through 4 give the results of profiles

dimensions as predicted from finite element simulation compared to experimental measurements. Figure 2 shows the predicted and measured cross sectional shape of workpiece for oval and round pass when the roll gap is 6.5mm. Dotted lines represent the roll groove shape. The cross sectional area measured at room temperature will be inevitably smaller than the prediction because the surface layers oxidized by air are scaled off after experiment. Figure 2(a) shows that the predicted maximum spread exceeds and pass (cross sectional) area slightly the measured one. Figure 2(b) demonstrates that the incoming oval workpiece was slightly twisted along its length direction during rolling. The predicted cross sectional area, overall, is in agreement with the measured one for both passes.

Figure 3(a) compares the experimentally measured cross sectional oval shape with the predicted one when the reference roll gap was reduced to 2.5mm. It shows that the predicted maximum spread is larger than the measured one. However, this difference could be partly due to mistake in roll gap setting. And careful comparison of the oval groove profile with experimentally measured cross sectional shape of deformed workpiece shows that the roll gap in oval pass was slightly larger than 2.5mm during experiment. Hence, the height of workpiece became larger than the pass height of the oval groove. Consequently, the measured maximum spread could be smaller than the predicted one. Figure 3(b) shows that the maximum spread predicted by FE simulation is slightly larger than that obtained by experiment.

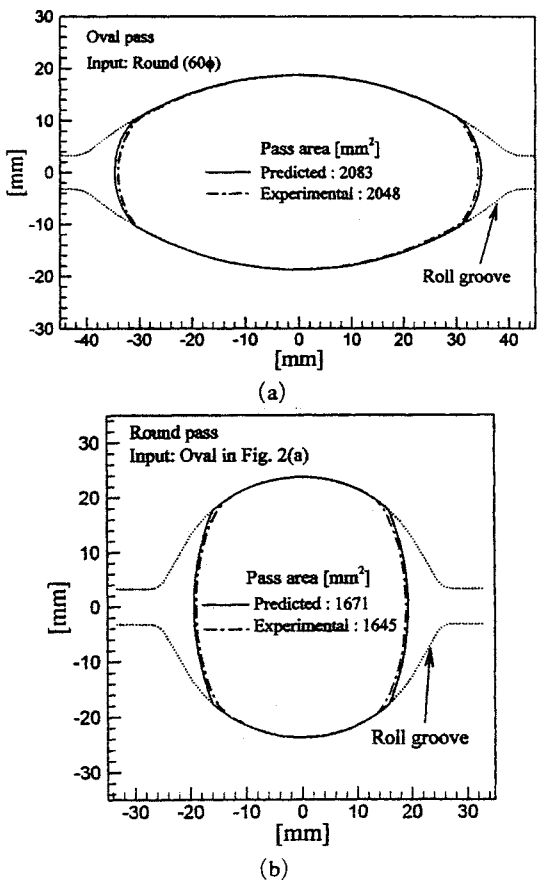

Fig. 2 Predicted and measured cross sectional shapes for the two-pass rolling (Fig. 1) when a bar with 60mm diameter is rolled

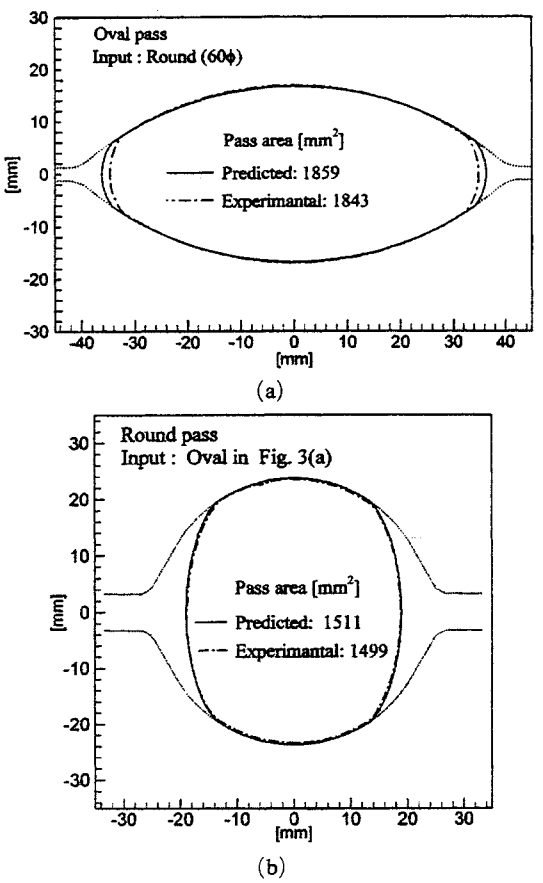

Fig. 3 Predicted and measured cross sectional shapes for the two-pass rolling (Fig. 1) when the roll gap of the oval groove reduced to 2.5mm

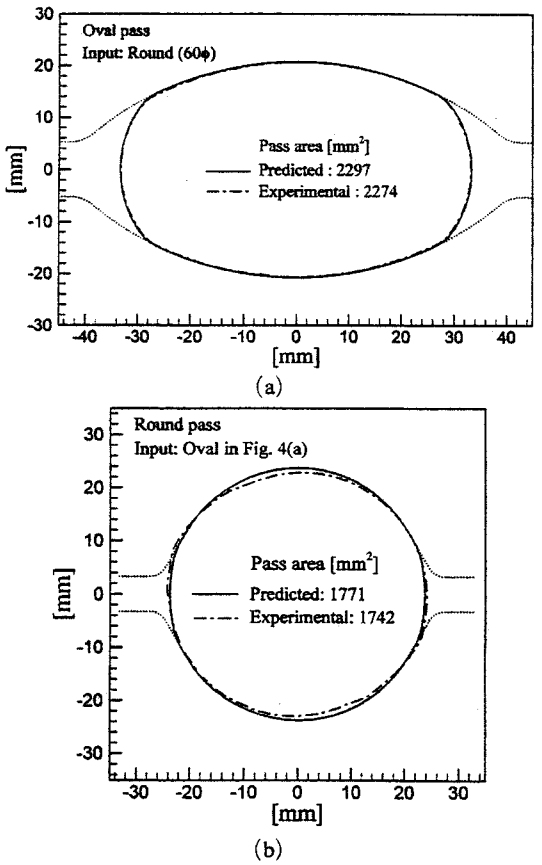

Fig. 4 Predicted and measured cross sectional shapes for the two-pass rolling (Fig. 1) when the roll gap of the oval groove increased to 10. 5mm

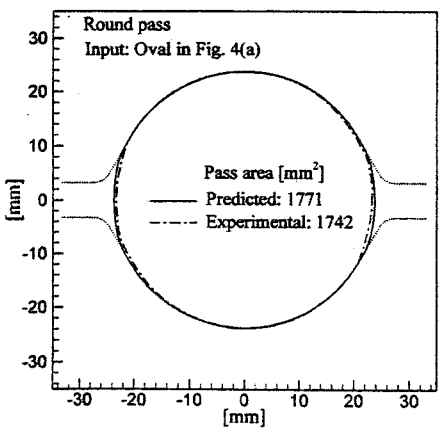

Fig. 5 Predicted and measured cross sectional shape of workpiece for the round pass rolling when a new entry guide is used at the ahead of round groove

But the predicted and measured pass (cross sectional) areas are in good agreement.

Figure 4 shows the predicted and measured cross sectional shape of workpiece for oval and round passes when the roll gap is 10.5mm. In Fig. 4(a) good agreement is noted between the predicted oval surface profile and the measured one. In Fig. 4(b), the measured cross sectional shape does not look like a round shape compared with the predicted one, which is almost a round shape. The workpiece in the round groove might have been twisted somehow along its length direction during rolling.

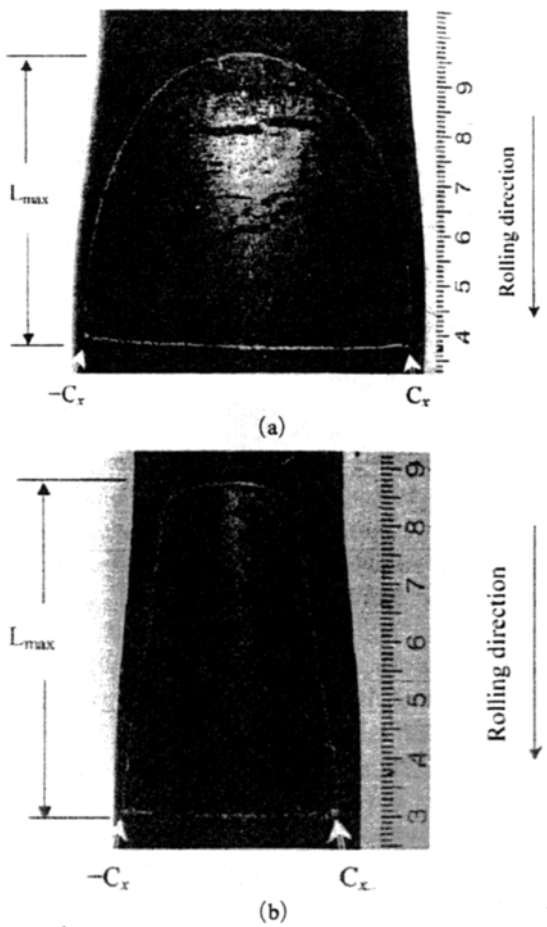

Fig. 6 Shape of projected contact area of workpiece deformed inside of roll groove and its geometric designation when a specimen with 60mm diameter is rolled. (a) Oval pass and (b) Round pass. The pass sequence is described in Fig. 1

To check the twist problem of workpiece, especially at round pass, during rolling, a new entrance guide was installed at the ahead of the round pass, which prohibited rotation of the workpiece during rolling. Figure 5 shows the predicted and experimentally measured cross sectional shapes when the new entrance guide was installed. As can be seen, almost a circular cross sectional shape was obtained from the experiment and the pass area was unchanged. This result shows that the workpiece in Fig. 4(b) was twisted during rolling as expected and demonstrates the importance of entrance guide especially at the ahead of the round pass in rod (or bar) rolling process.

To examine the model for the projected contact area in the analytical method, we obtained the projected area of contact between workpiece and roll groove surface, as shown in Fig. 6(a) and (b), for oval and round passes, respectively. These were acquired by the emergency stop of the pilot rod rolling mill and the pass sequence used is described in Fig. 1. The white line distinguishes the portion in contact. Here, C_x and $-C_x$ are points on the abscissa where the roll groove and deformed workpiece are separated (see Fig. 6). L represents the distance of the projected contact area to the rolling direction.

5.2 Exit velocity and forward slip of workpiece

Instrumentation for accurate measurement of workpiece exit velocity was not available. The input for the analytical method and finite element method is listed in Table 1. The calculated workpiece exit and entrance velocities for different pass sequences (pass1, pass2 and pass3) are shown in Table 2. It shows that the workpiece velocity from analytical solution is higher than that obtained from FE simulation, which may be due to the difference in modeling of friction behavior at the material/roll interface, which would affect forward slip (Magnus, 1988). The analytical analysis employed constant shear friction model while FE analysis used Coulumb friction model.

Again from Table 2, the centroid height e, for

Table 1 Variation of workpiece velocity at oval pass with varying roll gap

Pass sequence No.	1		2		3	
Oval pass gap(2g) mm	10.5		6.5		2.5	
Pass profile	Oval	Round	Oval	Round	Oval	Round
Outer roll radius r_o mm	155	155	155	155	1155	155
Inner roll radius r_i mm	139.5	134.5	139.5	134.5	139.5	134.5
Roll center distance r_c mm	160.25	158.25	158.25	158.25	156.25	158.25
Angular velocity ω/s	3.56	3.56	3.56	3.56	3.56	3.56

Table 2 Analytical solution and FE solution:

Pass sequence No.	1		2		3	
Oval pass gap(2g) mm	10.5		6.5		2.5	
Pass profile	Oval	Round	Oval	Round	Oval	Round
Analytical solution:						
Centroid height e mm	8.92	8.97	7.95	10.12	6.95	10.29
Neutral radius r_n mm	151.33	149.28	150.3	148.13	149.3	147.96
Exit velocity v_e m/s	0.539	0.531	0.535	0.527	0.532	0.526
Entry velocity v_o m/s	0.438	0.410	0.398	0.406	0.352	0.436
FE simulation:						
Exit velocity v_e m/s	0.513	0.514	0.528	0.501	0.545	0.493
Entrance velocity v_o m/s	0.413	0.402	0.390	0.403	0.359	0.400

which there is no slip, is below the workpiece contact level and therefore the entire surface of contact is subjected to backward slip. The variation of backward slip along the groove length of contact at the inner roll radius r_i defined as $s_i=(\omega r_i-v_i)/\omega r_i$, where v_i is the workpiece velocity at r_i, is shown in Fig. 7 for the three pass sequences as obtained from the analytical solution. Note that the x-direction is along the workpiece axis with the origin at the midpoint of the entry plane. The curves show that the minimum slip takes place in pass sequence No. 1 in which the round pass is completely filled. This pass also has, from Table 2, the minimum value of specific roll pressure, which means that it might provide the maximum groove life and hence it represents an optimum design. It is well known that roll wear which affects groove life is a function of roll pressure and the relative speed of roll and workpiece (Lundberg, 1993). Therefore, it should be important for process designers to design the rolling sequence such that the round pass is completely filled.

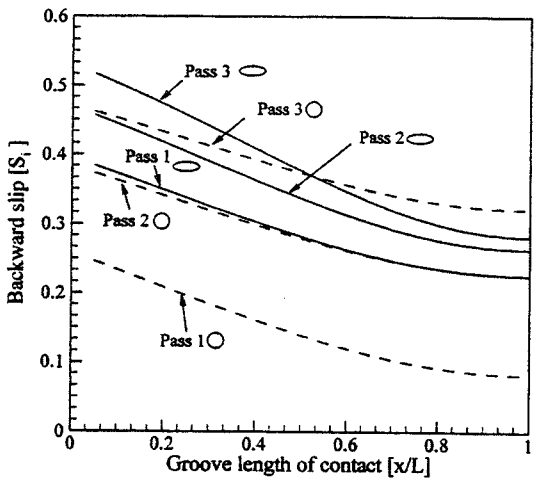

Fig. 7 Variation of backward slip along groove length of contact at $r=r_i$ obtained from the analytical solution

5.3 Stress, roll load and torque

The flow stress of workpiece was characterized by Shida's constitutive equation (Shida, 1969), giving the flow stress as a function of the carbon content, the strain, the strain rate and temperature. Shida's constitutive equation was chosen primarily due to its simplicity in applications. The flow stress of the workpiece (0.1%C, plain carbon steel) rolled at 1000℃ is then expressed as

$$\bar{\sigma}=150[1.658\bar{\varepsilon}^{0.403}-\bar{\varepsilon}]\dot{\bar{\varepsilon}}^{0.116}$$

Table 3 shows the values of roll load and torque, specific roll pressure, torque arm ratio and constant shear friction coefficient as obtained from analytical solution for different oval pass roll gaps. The stresses and roll torque were not

Table 3 Roll force and torque for different oval pass roll gaps

Pass sequence No.	1		2		3	
Oval pass gap(2g) mm	10.5		6.5		2.5	
Pass profile	Oval	Round	Oval	Round	Oval	Round
Experimental:						
Roll force P kN	271.3	232.9	381.8	202	458.3	187.4
Proj. contact area A_s mm^2			3036	1651		
Analytical:						
Coefficient c	−0.51	−0.04	−0.15	−0.38	0.34	−0.3
Coefficient q	0.479	0.661	0.693	0.606	0.908	0.693
Roll force P kN	273.6	233.3	380.6	203.2	459.5	185.4
Specific pressure p_s Mpa	116	113	133	128	136	124
Roll torque T kNm	12.14	10.88	19.43	9.77	26.53	9.38
Proj. contact area A_s mm^2	2354	2065	2857	1584	3391	1490
Roll length of contact L mm	50.8	49.88	56	53.52	60.8	57.6
Torque arm ratio a_r	0.441	0.467	0.456	0.449	0.475	0.439
Friction factor m	0.52	0.58	0.53	0.55	0.59	0.57

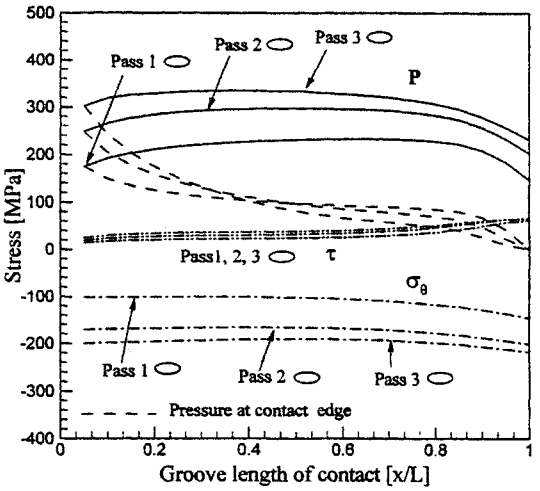

Fig. 8 Distribution of roll surface pressure P, shear traction τ and tangential stress σ_θ along the groove length of contact for the oval passes obtained from the analytical solution

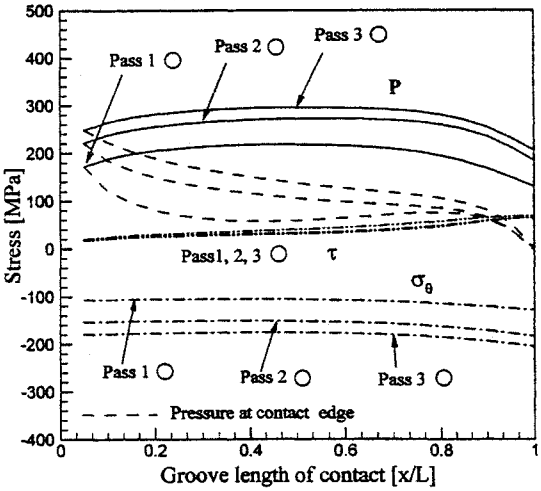

Fig. 9 Distribution of roll surface pressure p, shear traction τ and tangential stress σ_θ along the groove length of contact for the round passes obtained from the analytical solution

obtained experimentally since the instrumentation for their measurement was not available. The specific roll pressure and torque arm ratio are calculated as $p_s=P/A_s$ and $a_r=T/2PL$, respectively.

Table 3 indicates good agreement among roll load values as obtained from analytical results and experimental measurements. The predicted projected contact area slightly undervalues the measured one. The effect of oval pass roll gap on roll load and torque is more pronounced for the oval pass than for the round passes. The torque arm ratios are slightly higher than those commonly used in practice (Wusatowski, 1969), namely 0.4 for oval and 0.45 for round passes respectively.

The distributions of roll surface pressure **p**, shear traction τ and tangential stress σ_θ, along the groove length of contact at the inner roll radius, for oval and round passes are shown in Figs. 8 and 9, respectively, together with the roll surface pressure at the edges of the width of contact as obtained from analytical solution. Contrary to the usual distribution in flat rolling where there is a pressure peak in the vicinity of the neutral point at which the shear traction changes sign, the curves show an almost uniform distribution of the stresses at the groove root and the shear traction does not change sign. This is attributed to the curvature of the surface profile and the shape of the area of contact that allows equilibrium to be satisfied without a neutral point. The surface pressure at the edges of the width of contact, as shown by dotted lines, drops down along the direction of rolling reaching a zero value at exit. A comparison of the values of roll surface pressure at the inner roll radius with the value of specific roll pressure shows a high concentration of surface pressure at the groove root.

6. Concluding Remarks

This study has shown the effect of varying the roll gap of oval pass in round-oval-round pass rolling sequence on the interfacial slip along the groove contact surface and stresses that workpiece undergoes during rolling, using the analytical method and three-dimensional finite element method.

The results revealed that the entire surface of contact was subjected to backward slip during rolling. The stresses at the groove root had an almost uniform distribution along the length of contact with a high concentration of surface

pressure at the groove root. Optimum conditions in terms of minimum interfacial slip and minimum specific roll pressure, which may influence the maximum groove life, were obtained when the subsequent round pass is completely filled.

References

Arnold, R. R. and Whitton, P. W., 1975, "Spread and Roll Force in Rod Rolling," *Metals Technology*, Vol. 2, pp. 143~149.

Bayoumi, L. S., 1998, "Flow and Stresses in Round-Oval-Round Roll Pass Sequence," *Int. J. Mech. Sci.*, Vol. 40, pp. 1223~1234.

Kim, H. J., Kim, T. H. and Hwang, S. M., 2000, "A New Free Surface Scheme for Analysis of Plastic Deformation in Shape Rolling," *J. Mater. Proc. Tech.* Vol. 24 pp. 81~93.

Komori, K., 1997, "Simulation of Deformation and Temperature in Multi-Pass Caliber Rolling," *J. Mater. Proc. Tech.*, Vol. 71, pp. 329~336.

Lundberg, S. E., 1993, "A New High-Temperature Test Rig for Optimization of Materials for Hot-Rolling Rolls," *J. Mater. Proc. Tech.*, Vol. 36, pp. 273~301

Magnus, J., 1988, "Friction and Forward Slip in Hot Rolling," *Scan. J. Metall.*, Vol. 17, pp. 2~7.

Park, J. J. and Oh, S. I., 1990, "Application of Three Dimensional Finite Element Analysis to Shape Rolling Process," *J. Eng. Ind.*, Vol. 112, pp. 36~46.

Shida, S., 1969, "Empirical Formula of Flow Stress of Carbon Steels-Resistance to Deformation of Carbon Steels at Elevated Temperature," 2nd Report (in Japanese), *J. JSTP*, Vol. 10, pp. 610~617.

Shin, W., Lee, S. M., Shivpuri, R. and Altan, T., 1992, "Finite-Slab Element Investigation of Square-to-Round Multi-Pass Shape Rolling," *J. Mater. Proc. Tech.*, Vol. 33, pp. 141~154.

Tselikov, A., Nikitin, G. S. and Rokotyan, S. E., 1981, *The Theory of Lengthwise Rolling*, Mir Publisher, Moscow, pp. 133~139.

Wusatowski, Z., 1969, "Fundamentals of Rolling," Pergamon Press, Katowice, pp. 619~624.